Proteomic study of plaque fluid in high caries and caries free children

Weixu Chen[a], Zhiyan He[b,c], Shujun Ran[b], Jingping Liang[b] and Wei Jiang[b,*]

[a]*Department of Stomatology, Eye and ENT Hospital of Fudan University, Shanghai, China*
[b]*Department of Endodontics and Operative Dentistry, Shanghai Ninth People's Hospital, College of Stomatology, Shanghai Jiaotong University School of Medicine, National Clinical Research Center for Oral Diseases, Shanghai Key Laboratory of Stomatology, Shanghai, China*
[c]*Shanghai Research Institute of Stomatology, Ninth People's Hospital, School of Medicine, Shanghai Jiao Tong University, Shanghai, China*

Abstract.
BACKGROUND: The occurrence and development of caries is a complex process affected by multiple factor.
OBJECTIVE: The present study was envisaged to evaluate the plaque fluid in caries free children and children with high caries, in order to establish a data set of bacterial secretion proteomics. A non-labeled quantitative technique based on two-dimensional liquid chromatography-series mass spectroscopy was employed to detect plaque fluid. Based on the proteomics data, the database search, data processing and pathway analysis illuminated the function of these proteins, and clarified the role of plaque microecology in caries occurrence and development.
METHODS: The study enrolled 8 caries free (CF) children, whose decayed-missed-filled surface of teeth is 0 (dmfs = 0), and caries sensitive (CS) children, whose decayed-missed-filled surface of teeth is > 10(dmfs > 10) (3 ∼ 5 years old) for the smooth tooth plaque and the plaque in the high caries group. The plaque protein was extracted using the unlabeled quantitative technique like liquid chromatography-series mass spectrometry, using DeCyder[TM] MS Differential Analysis Software (version 1.0, GE Healthcare) that detected and compared the spectra, and quantified the full scanning before series mass spectroscopy. After obtaining all peptides with quantitative information, significantly differential polypeptide molecules were obtained ($p < 0.05$), and a metabolic pathway analysis was performed.
RESULTS: We identified 1,804 peptides with quantitative information, including 39 in CF, 30 in CS, and 1,735 similarly expressing peptides. After statistical analysis, 603 statistically different expression peptide data sets were obtained, including 202 high-expressed peptides in Group CF, 33 greater than 1.5 fold peptides, 401 high-expressed in Group CS and 199 greater than 1.5 fold peptide (173 nonredundant proteins).
CONCLUSION: Our study obtained the largest known dataset of the bacterial secretion protein in children with high caries, and screened the data set of high caries state. 603 peptides were statistically rich in 101 pathways, including glycolysis pyruvate acid metabolism, tricarboxylic acid cycle, pentyl phosphate pathway, fructose mannose metabolism, starch and sucrose metabolism, and ABC transporters.

Keywords: Proteomics, caries-free children, high caries children

1. Introduction

The occurrence and development of caries is a complex process affected by multiple factors, and reflects

---

the composition of microorganisms that is often not constant, but undergoes continuous dynamic changes. It also depends on the complexity of the interaction between the bacteria and the host. The functions within the plaque are not performed by a single individual organism, but involve the entire microbial community. However, in the current stomatology research, people's understanding of the micro-ecology is often based on the single microbial species purely cultivated in the laboratory, or the interaction of several limited species, and the understanding of the microbial community as a whole is far behind the understanding of its individuals.

The emergence of macroproteomics provides a good platform for a comprehensive research on the plaque protein components, but it is equally challenging. The first step of sample preparation, including the complete extraction of the bacterial intracellular and extracellular proteins in the plaque, is one of the major bottlenecks. In the extracellular environment where bacterial cells survive, the plaque fluid is the forefront of the bacteria interaction, host-specific and non-specific immunity, and is relatively easy for the separation and purification process, thereby being one of the ideal models for the research on caries. By analyzing the differences in the protein composition of the plaque in children without caries and those with high caries, the impact of between the plaque and host on the occurrence and development process of caries in children can be more intuitively and accurately explored.

To accomplish this, the study employed the non-labeled quantitative technology based on two-dimensional liquid chromatography-series mass spectrometry to analyze the plaque fluid in children without caries and children with high caries and established a data set of bacterial secretion proteomics. On this basis, using database search, data processing and pathway analysis, it further clarified the role of plaque microecology in the occurrence and development of caries.

2. Materials and methods

2.1. Sampling

According to the third version of the caries diagnosis standard of the Basic Methods of WHO Oral Health Survey, 8 children (CF, dmfs = 0) and CS, dmfs > 10 (3 $\sim$ 10) were selected respectively, without any oral diseases, systemic health, and no history of medication (including fluorogens) in March, 2020.

The children required no oral hygiene care on the night before sampling, starting from the morning, and 12 h fasting and drinking before sampling. Washing the collection area with sterile saline. Avoid moisture with cotton roll. In CF group, we scraped all the dental plaque of smooth suface of deciduous molar teeth. In CS group, we scraped all the healthy smooth enamel surface [1,2]. The parents of the child knowingly agreed for the experimental procedure.

2.2. Preparation of plaque sample

The plaque was collected in a pre-cooled 0.5 ml centrifuge tube in crushed ice and immediately sent to the laboratory and centrifuged at $4°C$, 15,000 g for 60 minutes to remove the bacteria, insoluble impurities and other substances, and the supernatant liquid obtained was the plaque fluid [3]. The plaque fluid was carefully transferred into the new EP tube, a protease inhibitor (Inhibitor cocktail complete, Roche) was added, and the concentrate was collected with the Millipore (cutoff: 5 KD) ultrafiltration tube at $4°C$, 4500 g. Quantitative protein concentration of the centrifugal fluid was done by Bradford (Bio-Rad, USA), and stored at $-80°C$ [4,5].
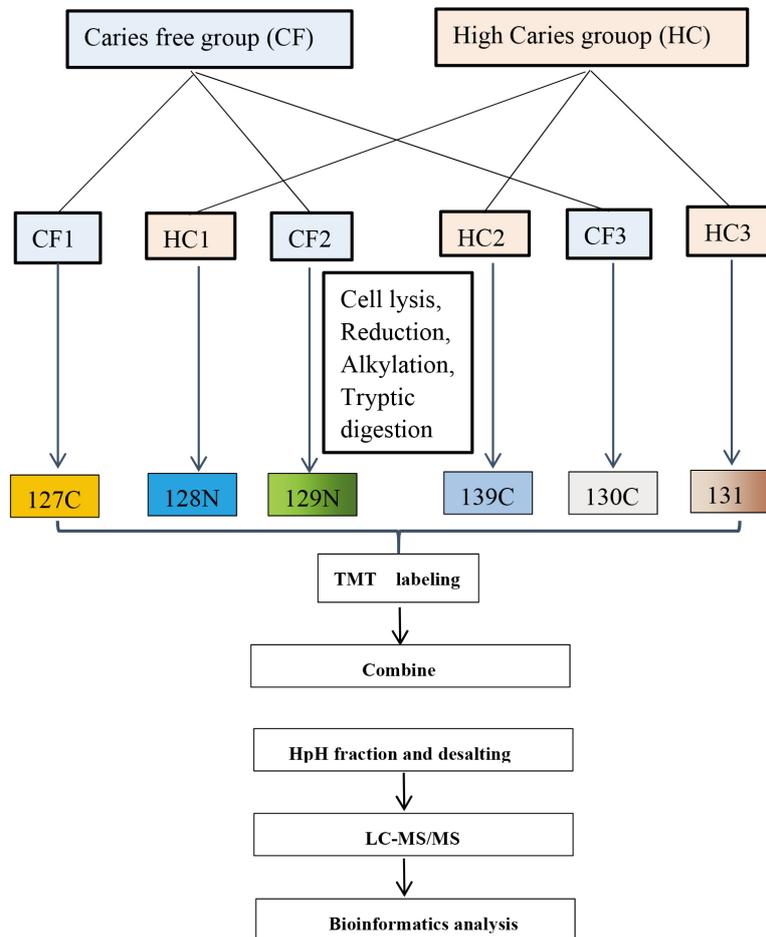
Fig. 1. Experimental workflow for TMT labeling and analysis: TMT 10-plex labeling was performed for three sets of technical replicates. Each condition was labeled as follows for the three technical replicates: CF (127N, 129N, 130C), HC (128N, 139C, 131). Moreover, equally amount of proteins from all samples were pooled as an internal standard (IS: 126). The labeled fractions were combined and subjected to High-pH Reversed-Phase Fractionation and desalting, followed by separation using liquid chromatography mass spectrometry (LC-MS/MS), and bioinformatics data analysis.

2.3. Preparation of enzyme solution

In order to reduce the differences between the individuals, the plaque proteins of the children without caries and children with high caries were mixed in equal amounts, and a sample library was established. CF and CS plaque were divided into three parts..Each protein samples were supplemented with lysis buffer (8 mol/Lurea, 40 mmol/L Tris, 65 mmol/L DTT) to the total volume of 100 μl, and mixed with 1 M DTT at 37°C for 2.5 hours. Subsequently, 10 μl 1 M IAA, was added at room temperature in absence of light and the reaction was continued for 40 minutes. After the above treatment, the protein was completely deformed, the disulfide bond opened up. It was then precipitated with a 5 x volume of precooled acetone (−20°C) by resting overnight (16 hours) at −20°C. Then, the mixture was centrifuged at 14,000 g for 40 minutes; the organic solvent was removed using pre-cooled acetone at −20°C, centrifuged again at 14,000 g for 40 minutes. To remove the salt ions, precooled 70% ethanol (−20°C) was added and
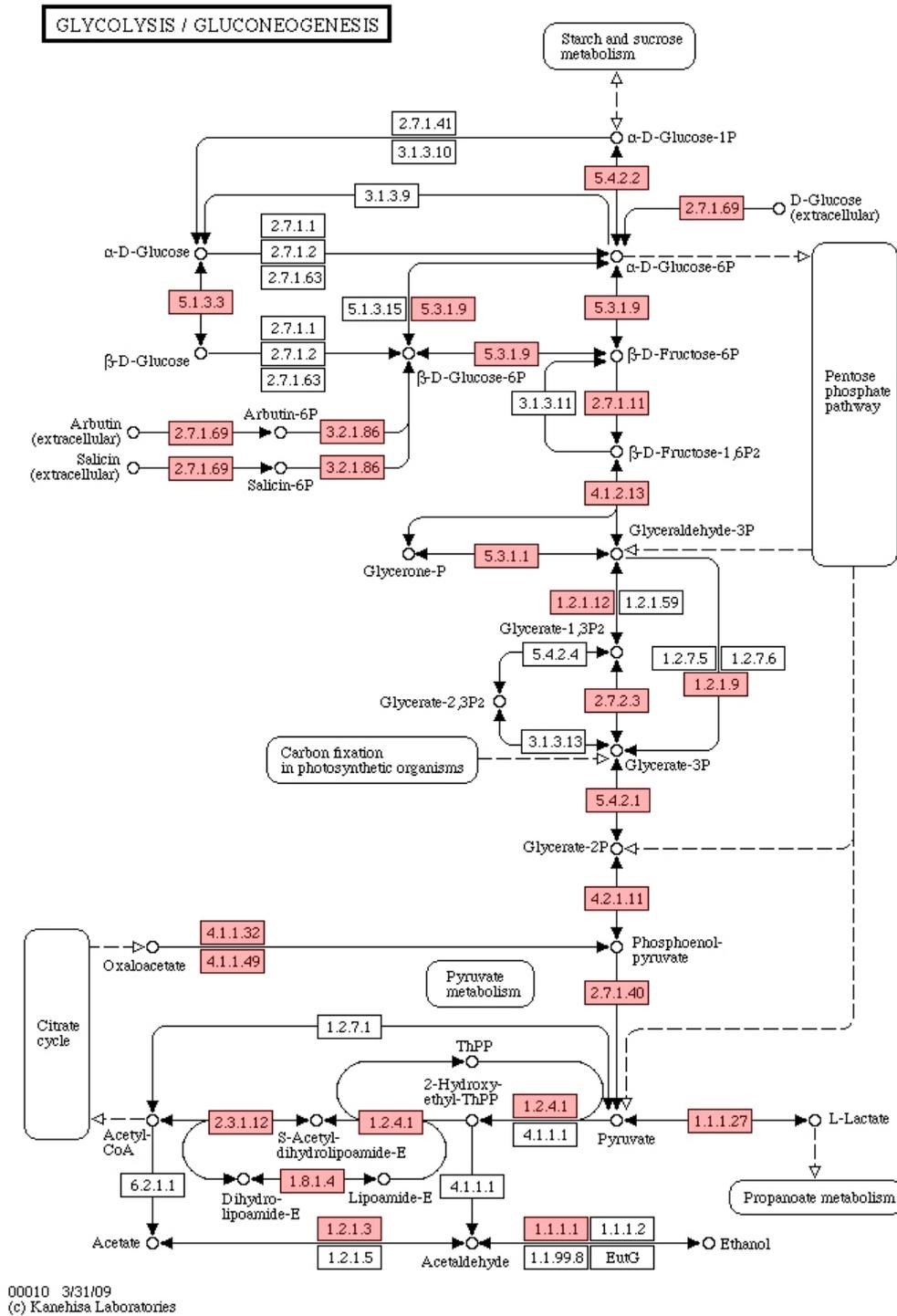
Fig. 2. Glycolysis/Gluconeogenesis.
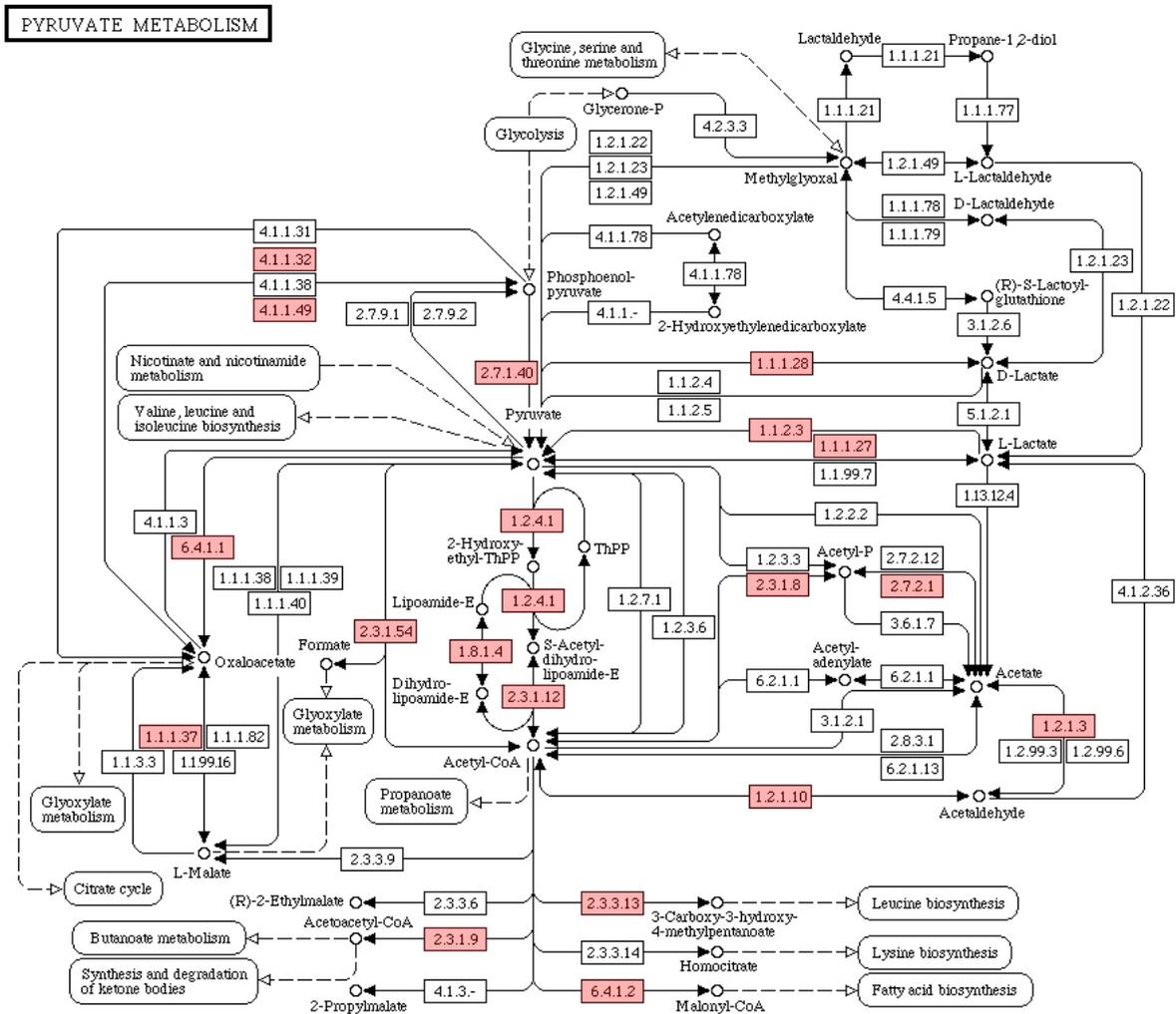
Fig. 3. Pyruvate metabolism.

centrifuged at 14,000 g for 40 minutes and then freeze dried. After the enzyme solution was completed, the ultrafiltration membrane was employed with Millipore 10 KD aperture size to collect the filter fluid and freeze dried at −80°C.

2.4. Liquid chromatography-mass spectrometry analysis

20 μg of the prepared enzyme solutions were taken and analyzed using the Ettan MDLC liquid chromatography-series mass spectroscopy system (GE Healthcare, Piscataway, NJ, USA). RP trap columns (Zorbax 300 SBC 18, Agilent Technologies, Palo Alto, CA, USA) were employed with an automatic sample feeder. The sample was desalted using the C18 trap column. The sample was separated on the C18 column (Millipore water in A phase and 0.1% FA 84% B finishing water solution, at a gradient
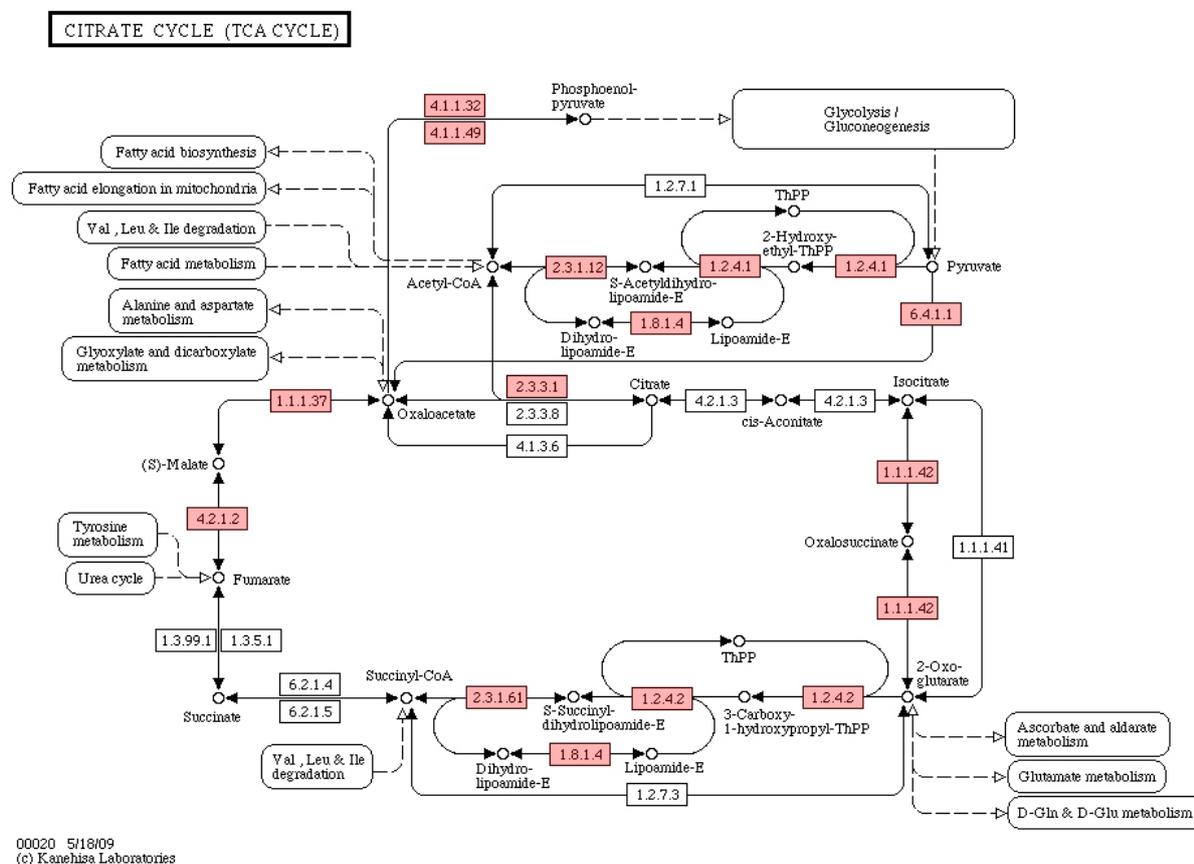
Fig. 4. Tricarboxylic acid cycle.

rising from 4% to 50% B phase within 2 hours). The separation speed was 2 μl/min. The samples were removed from the column, and subjected directly to electric spray source^{TM}LTQ^{TM}Linear ion-trap mass spectrometry (Thermo Electron, San Jose, CA, USA). The LTQ mass spectrometry was performed in the automatic gain control (AGC) mode, with the ion source parameters set as: electric spray voltage – 3.2 kV; capillary temperature – 170°C. Full-scan mass spectrograms were collected in the profile mode, while MS/MS maps were collected in the centroid mode, with 5 centroid mode scans after each profile mode. The analysis was repeated 3 times per sample.

2.5. Database search and data processing

After obtaining all peptides with quantitative information, It was tested for all $p < 0.05$, and searched with the SEQUEST program (Bioworks Browser Software suite, Thermo Electron, version 3.1) at the National Center for Biotechnology Information (www.ncbi.nlm.nih.gov) based on the genome information of 24 common oral bacteria in Genome. It was downloaded to get the corresponding protein sequence database (24 common oral bacteria including *Streptococcus gordonii* str. Challis substr. CH1, *Streptococcus mutans* UA159, *Streptococcus sanguinis* SK36, *Streptococcus salivarius* SK126, *Actinomyces odontolyticus* ATCC 17982, *Lactobacillus acidophilus*, *Lactobacillus fermentum*, *Neisseria mucosa* ATCC 25996, *Neisseria sicca* ATCC 29256, *Neisseria subflava* NJ9703, *Veillonella dispar* ATCC 17748,
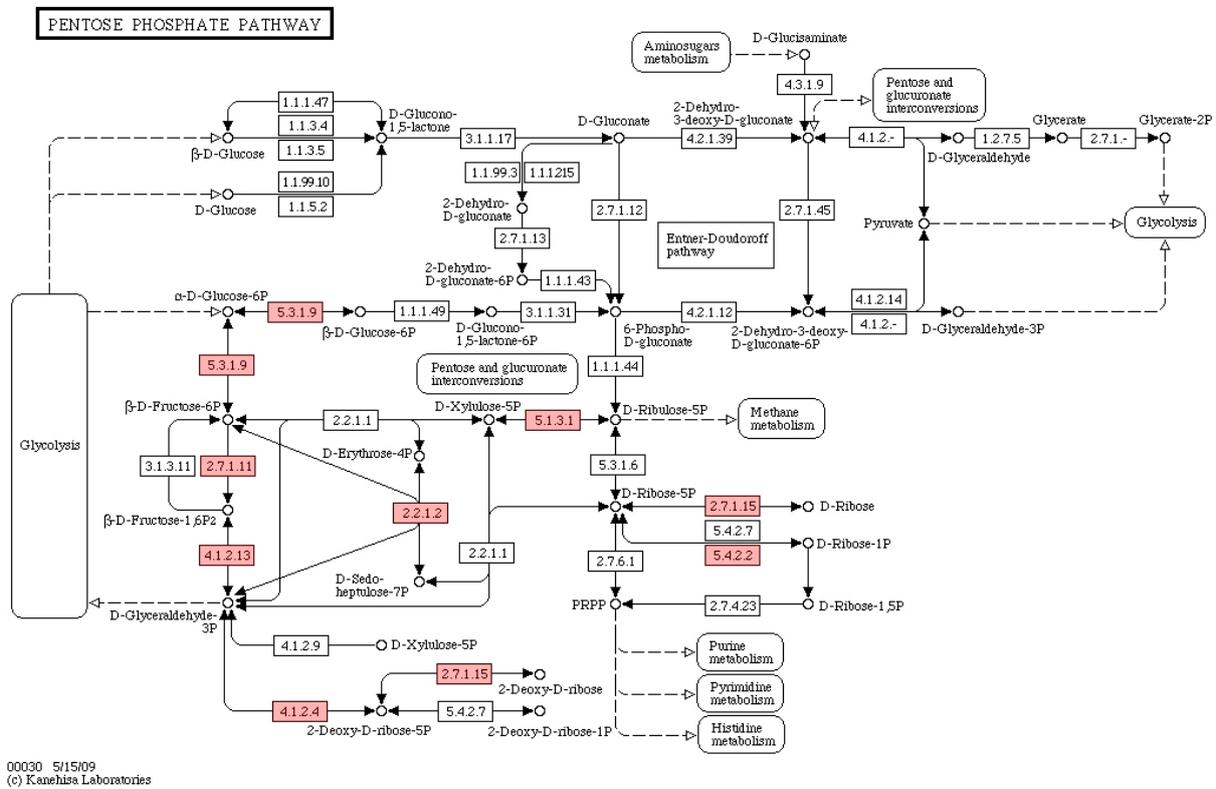
Fig. 5. Pentose phosphate pathway.

Veillonella parvula DSM 2008, *Corynebacterium matruchotii*, *Corynebacterium diphtheriae* NCTC 13129, *Leptotrichia buccalis* DSM 1135, *Eikenella corrodens* ATCC 23834, *Porphyromonas gingivalis*, *Prevotella melaninogenica* ATCC 25845, *Capnocytophaga gingivalis* ATCC 33624, *Capnocytophaga ochracea* DSM 7271, *Capnocytophaga sputigena* ATCC 33612, *Fusobacterium nucleatum*, *Treponema denticola* ATCC 35405, *Campylobacter rectus* RM3267). The polypeptide molecules were identified and their corresponding proteins were relatively quantified. The filter parameters were: when Charge $+$ 1, Xcorr $\geqslant$ 1.9; when Charge $+$ 2, Xcorr $\geqslant$ 2.2; when Charge $+$ 3, Xcorr $\geqslant$ 3.75; where DelCN $\geqslant$ 0.1.

2.6. Pathway analysis

The metabolic pathway map was downloaded for the 24 common oral bacteria from the www.kegg.com website to analyze the distribution of the identified proteins in each pathway.

2.7. Microbial function and pathway analysis

All identified microbial protein sequences were annotated by BLASTP (version: 2.2.31+) against the UniProtKB/Swiss-Prot database that included 560,118 sequences and the COG database (version: 2014) that included 1,781,653 sequences. Furthermore, InterProScan (version: 5.35–74.0) provided the gene ontology (GO) functional annotations of all identified microbial protein sequences with default parameters. Some in-house Perl scripts and R scripts were used to complete the GO functional classification and

Fig. 6. Fructose mannose metabolism.

statistics analysis. The KEGG orthology (KO) annotation of the proteins were performed using KOBAS (version: 3.0) with E-value$<=$1e-05 and rank$<=$5. Moreover, KOBAS was also used to perform a binomial test between the two groups in the KEGG pathway levels. Assignment of the proteins in the KEGG pathway levels was then visualized with Krona Excel Template.

2.8. PRM verification

Based on the results of the original label-free based quantitative meta-proteomics analysis, we selected the appropriate target peptides of the candidate proteins and performed targeted shotgun MS to finally determine the peptides of the target proteins with reliable identification information, which was used

Fig. 7. Fructose mannose metabolism.

in the PRM quantification analysis. The peptide information suitable for PRM analysis was imported into the Xcalibur software program for PRM setup. Briefly, 1 μg peptide from each sample was taken for LC-PRM/MS analysis. After sample loading, chromatographic separation was performed using a Thermo Scientific EASY-nLC nano-HPLC system. The following buffer was used: A solution was 0.1% formic acid aqueous solution and solution B was a mixed solution of 0.1% formic acid, acetonitrile, and water (95% of acetonitrile). The column was first equilibrated with 95% A solution. The sample was injected into a Trap column (100 μm × 20 mm, 5 μm-C18, Dr. Maisch GmbH) and subjected to gradient separation through a chromatography column (75 μm × 150 mm, 3 μm-C18, Dr. Maisch GmbH) at a flow rate of 250 nL/min. The liquid phase separation gradient was as follows: 0–25 minutes, linear gradient of B liquid from 5% to 18%; 25–45 minutes, linear gradient of B liquid from 18% to 50%; 45–48 minutes, linear gradient of B liquid from 50% to 95%; and 48–60 minutes, B liquid maintained at 95%. The peptides were separated and subjected to targeted PRM/MS using a Q-Exactive mass spectrometer (Thermo Scientific). The analysis time was 60 min. The parameters were set as follows: detection mode – positive; parent ion scanning range – 350–1500 m/z; capillary voltage – 1.8 kv; isolation width – 1.6 Th; first-order MS resolution – 70,000 @m/z 200; AGC target – 3e6; first-level maximum IT – 250 ms. Peptide secondary MS was performed as follows: for each full scan, target peptides of the precursor m/z were sequentially selected based on the inclusion list for second-order MS (MS2) scan with the parameters as follows: resolution – 35,000@m/z 200; AGC target – 3e6; Level 2 Maximum IT – 120 ms; MS2 Activation Type – HCD; Peptide fragmentation – nitrogen; Isolation window – 2.0 Th; Normalized collision energy – 28 eV. The obtained PRM data of the raw RAW file was analyzed using the Skyline 3.5

Table 1
High expression of bacterial secretory protein in plaque fluid of caries free children (> 1.5 fold)

NUM	Mass (Da)	Av. Ratio	Protein	ID Details
1	2019.2246	3.9419625	gi|34763016	Nicotinate-nucleotide pyrophosphorylase
2	1627.0841	3.9031119	gi|228274697	ISPg2, transposase
3	844.77333	3.1448998	gi|229211250	uncharacterized conserved protein
4	2015.8037	2.6245635	gi|228277090	competence protein
5	1308.9237	2.53298	gi|197736798	hypothetical protein FNP_1346
6	1485.0629	2.1089494	gi|213962598	ribosome recycling factor
7	1004.8306	1.965104	gi|223039105	selenium metabolism protein YedF
8	1583.1056	1.9346806	gi|229255033	predicted extracellular nuclease
9	1528.0214	1.9116673	gi|229211921	peroxiredoxin
10	1594.8706	1.8001297	gi|229255138	outer membrane protein
11	1369.6639	1.7949729	gi|34763038	NADH dehydrogenase reductase
12	1495.2313	1.793346	gi|188995429	hypothetical protein PGN_1565
13	1328.7801	1.7567087	gi|228275526	peptide chain release factor 2
14	1043.2649	1.7419186	gi|226710238	ribosomal protein L15
15	1289.2159	1.7255517	gi|229210576	chaperone protein DnaK
16	905.04655	1.6972979	gi|223039140	GTP-binding protein TypA/BipA
17	1814.3222	1.696517	gi|228277158	cell division protein FtsA
18	1341.9164	1.6860124	gi|229210533	glutamate dehydrogenase/leucine dehydrogenase
19	1614.0495	1.6716142	gi|223038584	carbamoyl-phosphate synthase, large subunit
20	1347.1639	1.6420553	gi|42527896	Jag protein, putative
21	1434.1841	1.6119828	gi|229210576	chaperone protein DnaK
22	1440.6899	1.6006457	gi|34762754	Alkyl hydroperoxide reductase C22
23	1583.0756	1.599004	gi|223039559	VirB10
24	1296.9619	1.5660363	gi|229210802	glyceraldehyde-3-phosphate dehydrogenase
25	1414.2779	1.561902	gi|229212600	LSU ribosomal protein L15P
26	1743.6774	1.5616289	gi|223039552	3-phosphoshikimate 1-carboxyvinyltransferase
27	1438.047	1.5568823	gi|238058718	Phosphoserine aminotransfera
28	913.14203	1.5564213	gi|229212593	LSU ribosomal protein L5P
29	714.50116	1.5434605	gi|229254206	outer membrane protein
30	888.51295	1.5399202	gi|229210548	fructose-bisphosphate aldolase
31	1254.5932	1.5356884	gi|223039512	phosphoribosylaminoimidazole carboxylase
32	1383.4912	1.5141757	gi|223038622	protein TolB
33	1366.1202	1.5058051	gi|213963395	putative outer membrane protein

software program. Statistical analysis was completed with R and the 'MetaboAnalystR' package.

Data availability: All the MS raw files were submitted to the Proteome Xchange Consortium (http://www.proteomexchange.com) via the PRIDE partner repository with the data set identifier.

2.9. Statistical analysis

Statistical analysis was performed using the SPSS version 19 software. The experiments were statistically analyzed with the independent sample T test. All statistical analysis were performed at 95% significance level using 2-tailed analysis.

3. Results

3.1. Label-free 2D-LC-MS/MS Identification

Liquid chromatography-series mass were analyzed in CF, CS group (we repeated the experiments for three times), including 1804 quantitative information peptides, 39 in CF group, and 30 in CS group. The
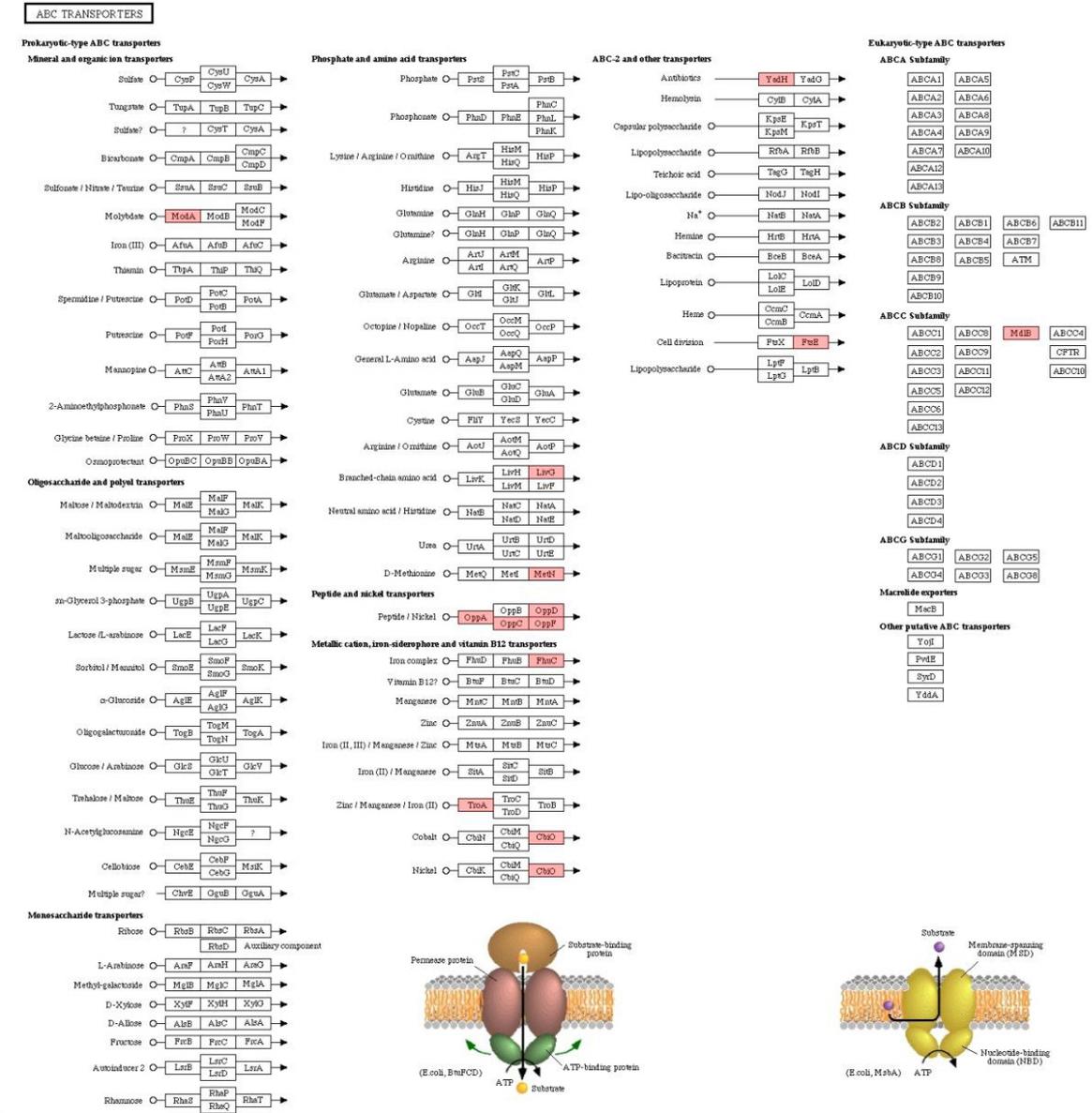
Fig. 8. ABC transport proteins.

$$C_6H_{12}O_6 + 2\ NAD^+ + 2\ ADP + 2\ H_3PO_4 \rightarrow 2\ NADH + 2\ C_3H_4O_3 + 2\ ATP + 2\ H_2O + 2\ H^+$$
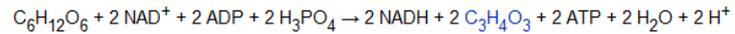
Fig. 9. Glycolysis reaction formula.

data from liquid chromatography-series mass spectroscopy was analyzed by DecyderMS software, and 603 peptide data sets were obtained, including 202 in CF group. Among them, 33 peptide has a much higher significant differences which was greater than 1.5 times (Table 1), On the other hand, we found

W. Chen et al. / Proteomic study of plaque fluid in high caries and caries free children

Table 2
High expression of bacterial secretory protein in plaque fluid of high caries children(> 1.5 fold)

NUM	Mass (Da)	Av. ratio	Protein	ID details
1	2968.55	14.07	gi|229210864	pyruvate kinase
2	1921.24	5.88	gi|225023847	hypothetical protein EIKCOROL_00713
3	1652.71	5.62	gi|223038968	GTP cyclohydrolase II
4	2016.63	4.81	gi|229211338	D-3-phosphoglycerate dehydrogenase
5	2463.40	4.80	gi|213964012	glyceraldehyde-3-phosphate dehydrogenase
6	2076.89	4.54	gi|229211633	bacterial nucleoid protein Hbs
7	1760.03	3.97	gi|228276851	signal transduction sensor histidine kinase
8	1702.16	3.60	gi|42526786	Fe-hydrogenase large subunit family protein
9	2008.27	3.29	gi|42527800	galactokinase, putative
10	1399.83	3.16	gi|229255924	glycosyltransferase
11	1767.07	3.14	gi|228274481	CobN/magnesium chelatase family protein
12	2283.30	3.00	gi|229210533	glutamate dehydrogenase/leucine dehydrogenase
13	1969.37	2.96	gi|229255585	conserved hypothetical protein YmdA/YtgF
14	2120.52	2.89	gi|229211673	aminotransferase [Leptotrichia buccalis DSM 11
15	1141.80	2.73	gi|42527828	cobyric acid synthase CobQ, putative
16	1420.06	2.68	gi|223039292	periplasmic nitrate reductase, large subunit
17	2206.43	2.68	gi|213962023	translation elongation factor Tu
18	1793.18	2.60	gi|228274858	alpha-glucosidase
19	1989.89	2.59	gi|229212231	Ser-tRNA (Thr) hydrolase; threonyl-tRNA synthet
20	1680.71	2.55	gi|34763824	Butyrate-acetoacetate CoA-transferase subunit B
21	2506.35	2.55	gi|229212304	Phospho-N-acetylmuramoyl-pentapeptide-transfer
22	2490.59	2.52	gi|229212655	theronine dehydrogenase-like Zn-dependent dehy
23	1848.55	2.52	gi|197737364	flavoprotein [Fusobacterium nucleatum subsp.
24	2545.12	2.45	gi|197736680	ESS family glutamate:sodium (Na+) symporter
25	2168.04	2.41	gi|42527533	OmpA family protein
26	1420.07	2.40	gi|229212277	galactose-6-phosphate isomerase lacB subunit
27	2550.84	2.36	gi|229210656	PTS system IIA component
28	2574.22	2.36	gi|229212275	tagatose-bisphosphate aldolase
29	2477.69	2.35	gi|228275593	glyceraldehyde-3-phosphate dehydrogenase, type I
30	2337.25	2.33	gi|228275800	translation elongation factor Ts
31	1390.89	2.28	gi|34763496	Transposase
32	1972.36	2.27	gi|228275746	All-trans-retinol 13,14-reductase
33	1893.57	2.26	gi|42525942	bacteriocin ABC transporter, bacteriocin-binding
34	1683.48	2.24	gi|42528037	hypothetical protein TDE2537
35	2116.25	2.22	gi|197735845	heat shock protein HtpG
36	1961.89	2.21	gi|229211604	glycerol dehydrogenase-like oxidoreductase
37	2130.66	2.21	gi|228274607	lysine–tRNA ligase
38	2056.26	2.20	gi|42525700	ABC transporter, ATP-binding protein
39	1595.09	2.19	gi|197735846	fructose-bisphosphate aldolase
40	1629.07	2.19	gi|229212489	Zn-dependent alcohol dehydrogenase
41	1747.08	2.18	gi|42525562	TPR domain-containing protein
42	2085.76	2.14	gi|188994038	probable transcriptional regulator AraC famil
43	2455.92	2.13	gi|188994275	thiol-disulfide interchange protein
44	1789.44	2.11	gi|229211224	2-isopropylmalate synthase
45	1753.58	2.11	gi|228275128	thiol-disulfide isomerase and thioredoxin
46	1565.07	2.10	gi|229212393	PTS system IIC component; diguanylate phosphod
47	1764.52	2.09	gi|223039902	methionine import ATP-binding protein MetN
48	1865.75	2.07	gi|228275077	2,3-bisphosphoglycerate-dependent phosphoglycerate
49	1873.80	2.06	gi|34762210	DNA integration/recombination/invertion protein
50	1716.11	2.06	gi|19703909	putative cytoplasmic protein
51	1608.73	2.05	gi|228274448	ribosomal protein S6
52	1938.30	2.04	gi|223039930	isocitrate dehydrogenase, NADP-dependent
53	2109.28	2.04	gi|34396499	hypothetical protein PG_0355

Table 2, continued

NUM	Mass (Da)	Av. ratio	Protein	ID details
54	1830.82	2.03	gi|34764184	Fructose-bisphosphate aldolase
55	2032.14	2.03	gi|229211623	aspartate semialdehyde dehydrogenase
56	2093.27	2.02	gi|34763916	Phage protein [Fusobacterium nucleatum subsp. v
57	1721.75	2.00	gi|225024749	hypothetical protein EIKCOROL_01635
58	2060.16	2.00	gi|34762309	Aspartate carbamoyltransferase
59	2051.33	1.99	gi|229210854	bacterial nucleoid protein Hbs
60	1689.00	1.99	gi|225025771	hypothetical protein EIKCOROL_02675
61	2109.08	1.99	gi|213962365	GDP-mannose 4,6-dehydratase
62	1984.14	1.99	gi|229210454	hypothetical protein LebuDRAFT_02810
63	1769.30	1.99	gi|229212758	DNA/RNA helicase, superfamily II, SNF2 family
64	1982.31	1.98	gi|34762754	Alkyl hydroperoxide reductase C22
65	1604.10	1.97	gi|225025378	hypothetical protein EIKCOROL_02276
66	2352.23	1.96	gi|229210734	nickel ABC transporter, periplasmic nickel-bin
67	1801.25	1.96	gi|229211277	triosephosphate isomerase
68	2169.29	1.94	gi|42525820	hypothetical protein TDE0304
69	1956.47	1.94	gi|42528183	RNA polymerase sigma factor WhiG
70	2003.22	1.92	gi|34763262	DNA helicase
71	1580.18	1.91	gi|213962986	conserved hypothetical protein
72	1634.89	1.90	gi|42526801	TldD/PmbA family protein
73	1813.18	1.89	gi|34762500	hypothetical protein
74	1473.49	1.89	gi|229256034	CRISPR-associated protein, Csn1 family
75	1917.00	1.88	gi|225025193	hypothetical protein EIKCOROL_02088
76	1764.27	1.88	gi|229212814	SSU ribosomal protein S30P
77	1695.78	1.86	gi|42525831	ABC transporter ATP-binding protein/peptidase
78	1892.92	1.86	gi|213962338	isocitrate dehydrogenase, NADP-dependent
79	1714.29	1.86	gi|213963684	probable transcriptional regulatory protein, C
80	1484.02	1.86	gi|229211130	glycogen/starch/alpha-glucan phosphorylase
81	1812.44	1.86	gi|228275794	conserved hypothetical protein
82	1759.24	1.85	gi|213962889	conserved hypothetical protein
83	1302.12	1.85	gi|229254579	hypothetical protein CochDRAFT_08810
84	1912.25	1.85	gi|213962806	apolipoprotein N-acyltransferase
85	1840.92	1.85	gi|197735467	ABC superfamily ATP binding cassette transpor
86	2159.33	1.84	gi|42526405	ABC transporter, ATP-binding protein
87	1523.07	1.83	gi|229211940	phosphoglycerate kinase
88	2126.30	1.83	gi|34762663	Phosphoglycerate kinase
89	1890.45	1.82	gi|228275464	isoleucine-tRNA ligase
90	2015.12	1.82	gi|34762786	CDP-glucose 4,6-dehydratase
91	1447.57	1.82	gi|229211563	uncharacterized conserved protein
92	1468.71	1.82	gi|34763070	tRNA (Uracil-5-) -methyltransferase
93	1811.06	1.82	gi|197736083	hypothetical protein FNP_0608
94	1769.04	1.81	gi|223038758	outer membrane lipoprotein
95	2322.33	1.81	gi|225024644	hypothetical protein EIKCOROL_01521
96	1898.96	1.81	gi|34762648	GTP-binding protein TypA/BipA TypA/BipA
97	1754.57	1.80	gi|213963724	dihydrolipoyl dehydrogenase
98	2038.83	1.80	gi|34762615	Hypothetical Cytosolic Protein
99	1804.83	1.79	gi|228276477	conserved hypothetical protein
100	1720.61	1.79	gi|197735629	hypothetical protein FNP_0141
101	1255.86	1.79	gi|223039442	ATP-dependent DNA helicase RecG
102	2159.84	1.78	gi|34764317	Flavodoxin
103	1949.98	1.77	gi|197736855	glutamate formimidoyltransferase
104	1735.95	1.77	gi|229210412	nonphosphorylating glyceraldehyde-3-phosphate
105	1417.96	1.77	gi|19703626	DNA polymerase III alpha subunit
106	2435.47	1.76	gi|225023733	hypothetical protein EIKCOROL_00597

Table 2, continued

NUM	Mass (Da)	Av. ratio	Protein	ID details
107	1952.19	1.76	gi|197735760	copper (Cu2+)-exporting ATPase
108	1946.13	1.75	gi|34762728	Enolase
109	2044.80	1.75	gi|228275814	fructose-bisphosphate aldolase, class II
110	2101.11	1.74	gi|225023349	hypothetical protein EIKCOROL_00207
111	1870.30	1.73	gi|188995942	mannose-1-phosphate guanylyltransferase
112	1815.15	1.72	gi|228275794	conserved hypothetical protein
113	2065.65	1.72	gi|229211517	sulfite reductase, beta subunit (hemoprotein)
114	2144.06	1.72	gi|229210391	signal transduction histidine kinase, COG0642
115	1444.38	1.72	gi|223038512	hypothetical protein CAMRE0001_0295
116	1681.92	1.71	gi|188995759	hypothetical protein PGN_1895
117	1946.32	1.70	gi|229211610	uncharacterized paraquat-inducible protein B
118	1982.21	1.70	gi|229212544	phosphoribosylformylglycinamidine synthase
119	1928.05	1.70	gi|213962314	hypothetical protein CAPSP0001_0185
120	2053.30	1.69	gi|42525700	ABC transporter, ATP-binding protein
121	1674.50	1.69	gi|229211928	Fe-S oxidoreductase
122	2025.65	1.68	gi|197737300	possible plasmid mobilization protein
123	2124.28	1.67	gi|229211402	D-isomer specific 2-hydroxyacid dehydrogenase
124	2205.30	1.66	gi|213963583	conserved hypothetical protein
125	1460.65	1.66	gi|42527134	glycine cleavage system H protein
126	1899.49	1.66	gi|188994568	putative tonB-linked outer membrane receptor
127	1541.42	1.66	gi|213963481	glycogen synthase
128	1887.21	1.64	gi|197736995	3-dehydroquinate synthase
129	1273.98	1.64	gi|228274891	conserved hypothetical protein
130	1657.53	1.63	gi|197736095	pyruvate synthase [Fusobacterium nucleatum su
131	1483.78	1.63	gi|229211272	hypothetical protein LebuDRAFT_11420
132	2134.60	1.62	gi|228276496	ribosomal protein S3
133	1618.98	1.62	gi|197736759	N-acyl-D-aspartate/D-glutamate deacylase
134	1782.11	1.61	gi|34397232	DNA-binding protein, histone-like family
135	1586.32	1.61	gi|42526652	phage minor structural protein, putative
136	1693.94	1.61	gi|197736825	hypothetical protein FNP_1373 [Fusobacterium
137	2148.12	1.61	gi|197735216	elongation factor EF1A
138	2002.16	1.61	gi|225025671	hypothetical protein EIKCOROL_02573
139	1480.44	1.60	gi|188994351	FtsK/SpoIIIE family cell division protein
140	1816.96	1.60	gi|19703982	putative cytoplasmic protein
141	1776.34	1.59	gi|42527210	hypothetical protein TDE1704
142	2021.76	1.59	gi|42526714	integrase/recombinase XerD
143	2098.43	1.59	gi|225024872	hypothetical protein EIKCOROL_01760
144	1480.96	1.58	gi|213964056	aspartyl-tRNA synthetase
145	1712.68	1.57	gi|213962204	hypothetical protein CAPSP0001_1551
146	1874.39	1.57	gi|225023233	hypothetical protein EIKCOROL_00085
147	1494.21	1.57	gi|229210434	UDP-N-acetylmuramyl tripeptide synthase
148	1673.82	1.56	gi|19705272	4-amino-4-deoxychorismate lyase
149	1951.21	1.56	gi|42525731	TPR domain-containing protein
150	2204.99	1.56	gi|228274869	chaperone protein DnaK
151	1590.11	1.56	gi|188993943	hypothetical protein PGN_0079
152	1601.16	1.56	gi|42527320	hypothetical protein TDE1814
153	1889.49	1.56	gi|42528104	hypothetical protein TDE2604
154	1664.98	1.55	gi|223039847	fructose-1,6-bisphosphatase
155	1377.94	1.55	gi|34764886	Export ABC transporter
156	2059.94	1.55	gi|34762866	hypothetical protein
157	2792.72	1.55	gi|229212597	LSU ribosomal protein L18P [Leptotrichia bucca
158	1143.01	1.55	gi|229212654	hypothetical protein LebuDRAFT_25250
159	1772.95	1.54	gi|228276146	hypothetical protein CAPGI0001_0708
160	1601.40	1.54	gi|188995090	ribonucleotide reductase

Table 2, continued

NUM	Mass (Da)	Av. ratio	Protein	ID details
161	1885.91	1.54	gi|42527008	hypothetical protein TDE1500
162	1999.21	1.54	gi|42527772	methyl-accepting chemotaxis protein
163	1859.62	1.54	gi|229212449	McrBC 5-methylcytosine restriction system comp
164	1423.17	1.53	gi|229255650	hypothetical protein CochDRAFT_19730
165	2024.66	1.53	gi|229210424	alpha-phosphoglucomutase
166	1603.16	1.53	gi|213963535	conserved hypothetical protein
167	2136.53	1.52	gi|197736694	hypothetical protein FNP_1239
168	2170.12	1.52	gi|213962656	conserved hypothetical protein
169	1958.17	1.52	gi|225023180	hypothetical protein EIKCOROL_00032
170	1441.73	1.52	gi|229255214	protease subunit of ATP-dependent protease
171	1786.80	1.51	gi|18463955	replication protein
172	1655.44	1.51	gi|42526889	V-type ATP synthase subunit E
173	1460.62	1.51	gi|34762313	Carbamoyl-phosphate synthase large chain

401 peptide in CS group. And there were 199 among them has a greater differences which more than 1.5 times (173 without redundant proteins, Table 2).

3.2. Gene ontology function analysis

In total, 9194 (80.16%) identified microbial leading proteins corresponded to at least one GO term using InterProScan and in-house Perl Scripts. The number of proteins was counted at GO level 2 of biological process, cellular component, and molecular function ontology, respectively (Fig. 7). Moreover, the proteins of two groups that corresponded to the GO term of biological process, cellular component, and molecular function ontology were counted. Then, Fisher's exact test was performed to compare the difference of the protein group number between the two groups. Based on a $p < 0.05$ level, the GO terms with CS group included 35 in biological process ontology, 2 in cellular component, and 30 in molecular function ontology. The GO terms with CF group included 59 in biological process ontology, 17 in cellular component, and 30 in molecular function ontology (Fig. 8).

The count of proteins corresponding to GO terms of all samples were performed using in-house Perl and R scripts. With a $p < 0.05$, 80 GO terms (33 in biological process ontology, 5 in cellular component ontology, and 42 in molecular function ontology) were found in atleast12 pair samples with high caries, while only 10 GO terms (8 in biological process ontology and 2 in molecular function ontology) were found in the caries-free specimen. Then, we transformed the p-value with negative log10, and visualized them with heatmaps using R (Fig. 9).

3.3. PRM verification

Parallel reaction monitoring (PRM) mass spectrometry was used to verify the target peptides determined by the metaproteomic analysis and a pre-experiment, and the 171 candidate peptides of the target protein were subjected to LC-PRM/MS analysis. In total, 103 candidate proteins were quantified by LC-PRM/MS, including 3 proteins (hinf_c_1_1270, fnuc2539_c_1_361, cgin_c_10_1771) that were determined as the differential expressed protein candidates in the metaprotemics study. The Skyline analysis results of each candidate peptide were shown.

Meanwhile, 17 differential expressed peptide candidates were confirmed by the Mann-Whitney U test with a $p < 0.05$ cutoff, 15 differential expressed peptide candidates were obtained by paired-samples T test with a $p < 0.05$ cutoff, and 7 peptides in common (Table 6).
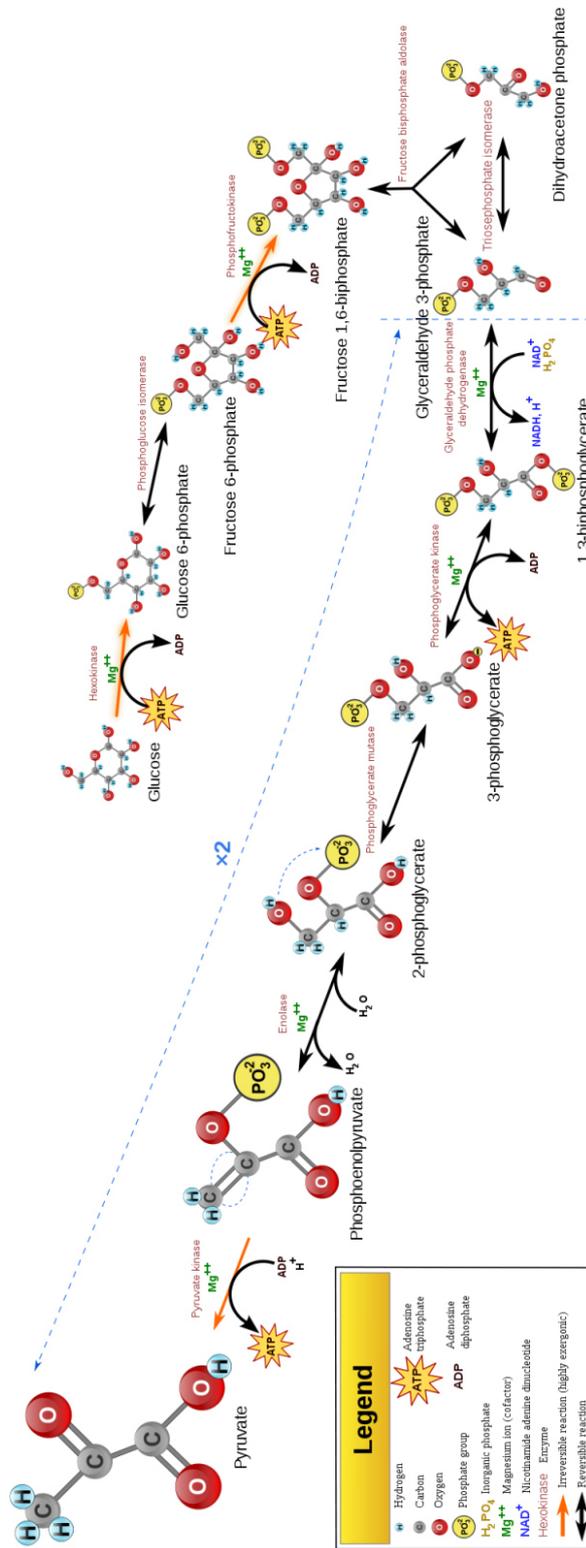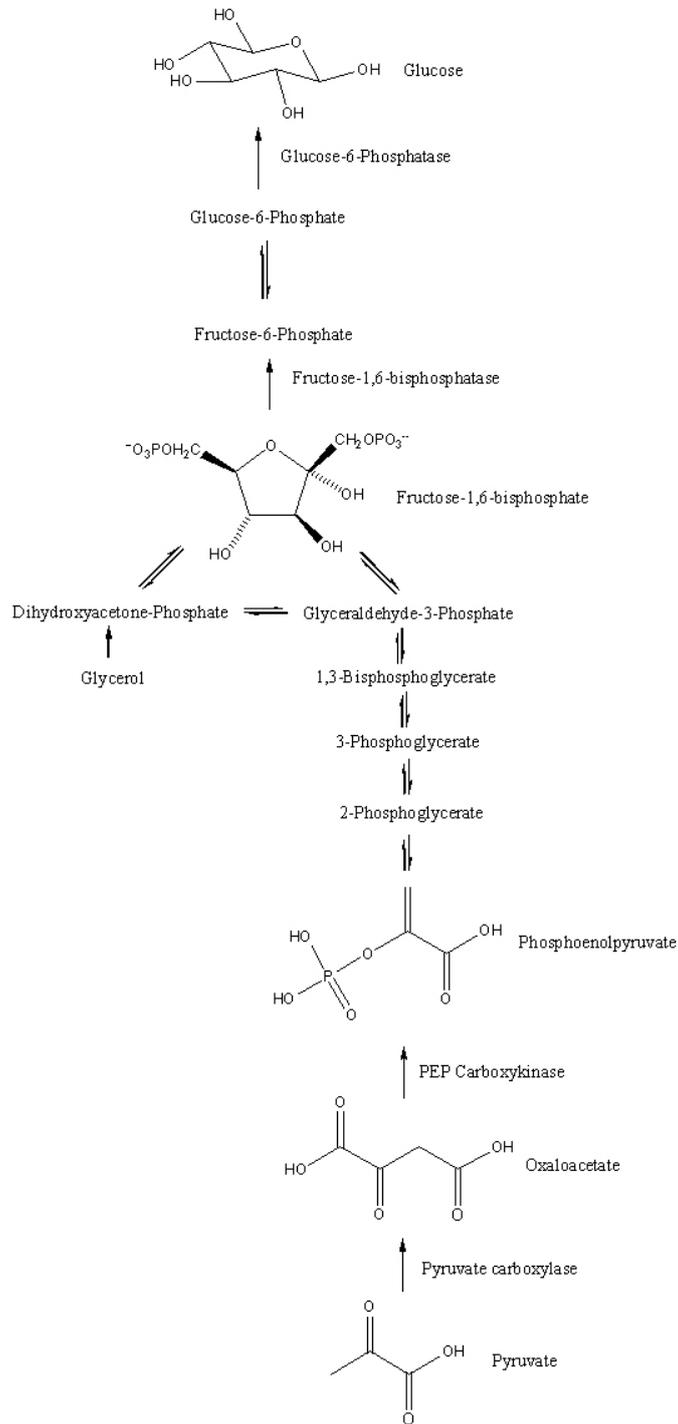
Fig. 10. Glycolysis.

Fig. 11. Gluconeogenesis.

Table 3
High expression ABC transporter data set of CS group ($P < 0.05$)

Num	Ratio	GI ID	ID details
1	2.26	gi|42525942	bacteriocin ABC transporter, bacteriocin-binding
2	2.20	gi|42525700	ABC transporter, ATP-binding protein
3	1.96	gi|229210734	nickel ABC transporter
4	1.86	gi|42525831	ABC transporter ATP-binding protein/ peptidase
5	1.85	gi|197735467	ABC superfamily ATP binding cassette transporter
6	1.84	gi|42526405	ABC transporter, ATP-binding protein
7	1.69	gi|42525700	ABC transporter, ATP-binding protein
8	1.55	gi|34764886	Export ABC transporter
9	1.44	gi|197735439	ABC superfamily ATP binding cassette transpor
10	1.37	gi|34763755	ABC transporter ATP-binding protein
11	1.39	gi|229211590	ABC-type metal ion transport system
12	1.19	gi|34763045	ABC superfamily ATP binding cassette transpor
13	1.12	gi|34763548	Hemin transport system ATP-binding protein hmuV

Table 4
High expression ABC transporter data set of CF group ($P < 0.05$)

Num	Ratio	GI ID	ID details
1	1.32	gi|229210852	ABC-type uncharacterized transport system
2	1.26	gi|188994222	putative ABC transporter ATP-binding protein
3	1.18	gi|42525832	ABC transporter, ATP-binding/permease protein
4	1.16	gi|34763794.1	branched chain amino acid ABC superfamily ATP

4. Discussion

In this study, we initially used the method of macroproteomics to find the bacterial secretion proteins in caries-free children and children with high caries, with a total of 1735 peptides, including 603 statistically different peptides. Further bioinformatics study found that the proteins with differences in the expression were more than 1.5 times mainly concentrated in the glycolysis/glyneogenesis, pyruvate metabolism, citric acid circulation, ABC transporters, etc. We will discuss from two aspects – the pathways and the key proteins.

4.1. Saccharolysis/sugar lyiogenesis

4.1.1. Glycolysis

Saccharolysis (glycolysis) is the first step in the sugar metabolism process of all biological cells. During this process, a molecule of glucose undergoes a ten-step enzyme reaction to form two molecules of pyruvate with the formation of ATP (Figs 8–10). This suggests the presence of active sugar metabolism in the caries-causing plaque, presumably due to the highly expressed enzymes that use intracellular polysaccharide, mainly glycogen as a source of energy, resulting in tooth demineralization [6].

Phosphorylation of the phosphoric fructose (phosphorylation of fructose-6-phosphate) is the third step of glycolysis, further phosphorylation of C on 6-phosphate fructose initially produces 1,6-diphosphate fructose supplied by ATP. The reaction is catalyzed by phosphate fructose kinase (phosphofructokinase, PFK), which is an important speed limiting enzyme in the sugar aerobic oxidation process. Phosphoric transfer of phosphoenol pyruvate is the final reaction in glycolysis that involves the transfer of the high energy phosphorate group from phosphoroll pyruvate to ADP, and is catalyzed by pyruvate kinase, PK, which is another phosphorylation process at the substrate level.
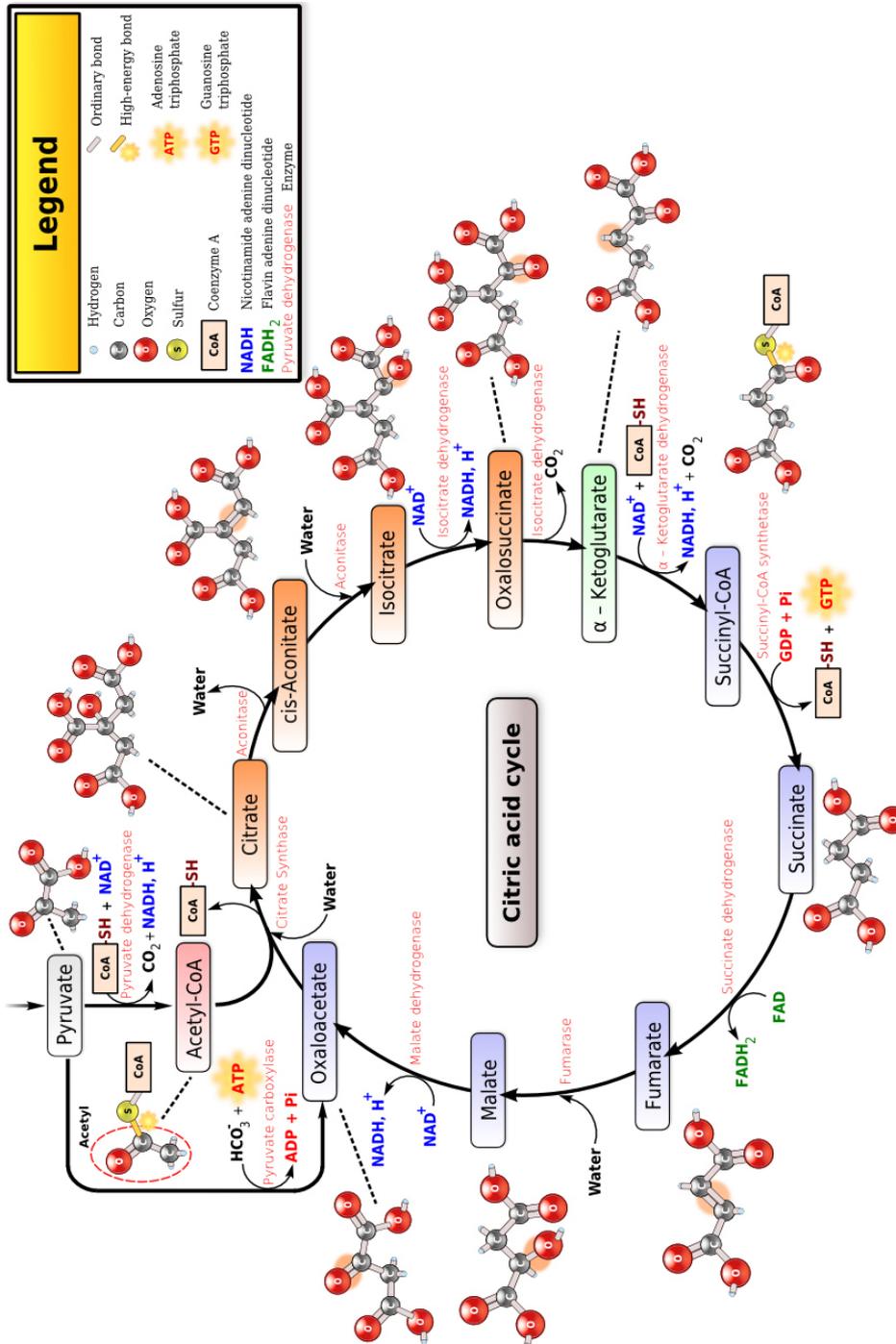
Fig. 12. Tricarboxylic acid.

Table 5
Co expression ABC transporter data set of CS&CF group ($P > 0.05$)

Num	GI ID	ID details
1	gi|197735467	ABC superfamily ATP binding cassette transport
2	gi|229212097	ABC-type multidrug transport system
3	gi|229212809	ABC-type multidrug transport system
4	gi|229210643	ABC-type oligopeptide transport system
5	gi|42527941	ABC transporter, ATP-binding/permease protein
6	gi|229211946	ABC-type cobalt transport system
7	gi|229211911	ABC-type Fe^{3+} transport system
8	gi|229211590	ABC-type metal ion transport system
9	gi|42526433	ABC transporter, ATP-binding/permease protein
10	gi|42528282	ABC transporter, ATP-binding/permease protein
11	gi|42525789	ABC transporter, ATP-binding/permease protein
12	gi|42526418	ABC transporter, ATP-binding protein
13	gi|42526693	ABC transporter, ATP-binding protein
14	gi|42525831	ABC transporter ATP-binding protein/peptidase
15	gi|229210567	amino acid/amide ABC transporter membrane prot
16	gi|19704374	branched chain amino acid ABC transporter
17	gi|197736157	dipeptide/oligopeptide/nickel (Ni^{2+}) ABC supe
18	gi|228274621	excinuclease ABC subunit A
19	gi|42526877	excinuclease ABC subunit B
20	gi|42527978	excinuclease ABC, C subunit
21	gi|42527718	galactoside ABC transporter, ATP-binding protein
22	gi|197736905	iron (Fe^{3+}) ABC superfamily ATP binding casse
23	gi|42526259	iron compound ABC transporter
24	gi|42526690	iron compound ABC transporter
25	gi|197736077	nickel (Ni^{2+}) ABC superfamily ATP binding cas
26	gi|197736393	possible nitrate/sulfonate/bicarbonate ABC su

Table 6
Candidate differential expressed peptides were confirmed by Mann-Whitney U test and paired-samples T test in common

Peptide sequence	p-value with Mann-Whitney U test	p-value with paired-sample T test	Fold change
VVEYVEKPVIVYR	4.90E-02	4.63E-02	8.51
YSFSTCYNSER	3.56E-03	4.40E-03	5.21
TAALENAAEGGFNKK	2.19E-02	5.22E-03	4.33
VVVEVLSQGK	2.27E-02	5.87E-03	3.73
LNNCPTSPR	4.35E-02	3.32E-02	3.71
VLDELTALR	4.97E-02	4.18E-02	2.50
SPEEAYEHAK	4.91E-02	2.51E-02	2.14

Reversible reactions in glycolysis include 7 steps: glucose phosphate isomerase is involved in the second step; heterogeneous reaction of glucose phosphate (isomerization of glucose-6-phosphate); participation in step 4 1.6-diphosphate pyrolysis reaction (i.e. cleavage of fructose 1, 6 di/bis phosphate from fructose-1, 6-Bisphosphate Aldoase (fructose-1, 6-bisphosphate aldolase); participation in step 6: 3-glyceraldehyde phosphate oxidation reaction (oxidation of glyceraldehydes-3-phosphate); 3-glyceraldehyde phosphate dehydrogenase (glyceraldehyde 3-phosphate dehydrogenase); phosphorate kinase (phosphoglycerate kinase, PGK) participating in high energy phosphate bond transfer of step 1.3-diphosphate glyceric acid. These enzymes showed a high expression in the plaque fluid in both two groups. Studies show that the above catalytic enzymes participate in the sugar heterogeneous reaction at the same time. So, we speculate that both in caries-free or caries causogenic plaque, the glycolysis and sugar heterogeneous reaction can be accurately adjusted, so that the bacteria in the plaque can use the excess sugar in the form of glycogen as energy storage to meet their own energy needs.
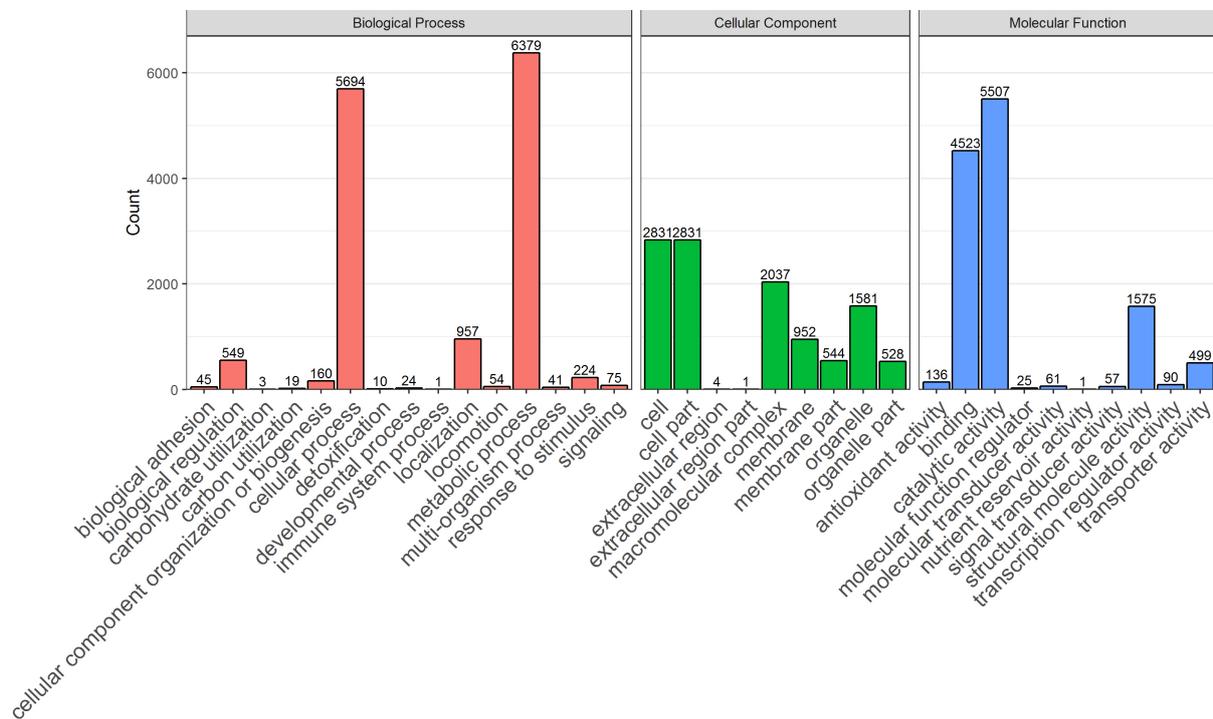
Fig. 13. A bar chart of protein count at GO level 2 of biological process, cellular component, and molecular function ontology using the 'ggplot2' package. The number markers at the bar were protein count of the GO term.

The final reversible reaction is step 2-phosphoglyceric acid, catalyzed by enolase, which was highly expressed in the CS group ($P < 0.05$, ratio = 1.75), and mainly corresponds to the bacterial glycolysis pathway, suggesting that glycololysis plays an extremely important role in carie.

4.1.2. Gluconeogenesis and NAD⁺ regeneration

There are three-step reactions in glycolysis that are irreversible reactions that must be bypassed during sugar heterogenesis, at the cost of higher energy consumption (Fig. 11). The fructose-1,6-diphosphatase involved in this process was highly expressed in the CS group and the phosphoenlate-type pyruvate carboxylated kinase was expressed in both groups, suggesting that the sugar heterogenesis occured in both the mature and the pathogenic plaque and was precisely regulated.

NAD⁺ can be regenerated by lactate dehydrogenase (lactate dehydrogenase, LDH), ethanol dehydrogenase (Alcohol dehydrogenase, ADH), and NADH dehydrogenase. LDH is the key enzyme for synthetic lactic acid, and its biological effect is the key link in causing caries. *S. mutans* lacking LDH activity significantly reduced the caries *in vivo* in the restricted rodent model experiments [7–9]. However, there was no significant difference in the mean LDH activity of *S. mutans* in different caries-sensitive populations [10]. This experiment also found no significant difference in the LDH expression in children with no or high caries. But the lack of LDH has a lethal effect on the bacteria, since an LDH deficient strain results in intracellular NAD during aerobic growth⁺/NADH metabolic imbalance and accumulation of glycolysis toxic intermediates, killing the bacteria. The results of this experiment in turn confirms the idea that, whether there is caries or the absence of caries, there must be an active expression of LDH, which is one of the necessary conditions for the *Streptococcus* bacteria to survive.

4.2. Tricarboxylic acid circulation

The cytoplasm of prokaryotes is the site of tricarboxylic acid circulation, but most enzymes are found in plaque fluid, including isocitrate dehydrogenase (isocitrate dehydrogenase, IDH) (Fig. 12), succinate dehydrogenase, malate dehydrogenase, succinyl-assisted A synthase, and α-ketovaltarate dehydrogenase complex in the CS group are unknown.

The IDH superfamily is ancient and large, widespread in the three boundaries of life (archaea, bacteria and eukaryotes). IDH catalyzes isocitric acid to α-ketopenta in tricarboxylic acid (TCA) cycle, bringing NAD^+ or the $NADP^+$ to NADH or a NADPH. It not only plays an important role in energy metabolism, amino acids and vitamin synthesis, but also plays a key regulatory role in the TCA circulation and the carbon flux distribution of acid bypass [11–14].

4.3. ABC transporter protein

This study identified more than 50 corresponding adenosine triphosphate binding box transporters (ATP-binding cassette transporter, ABC transporters) in children who were caries-free or with high caries. Associated with the transport of iron, nickel, cobalt ions, iron compounds, metal ions, oligopeptides, dipeptides, amino acids, branched chain amino acids, lactosidase, it is seen that ABC transporters are involved in various physiological functions of bacteria. It is worth noting that we identified 13 highly-expressed ABC transporters in the CS group, 6 proteins expressed more than 1.5 times, while only 4 ABC transporters were highly expressed in the CF group and all were less than 1.5 times, suggesting that material transformation in the process of caries-causing transformation of bacteria. Among them, ABC transporter of the group CS was expressed 2.6 times high, which may be the potential target molecule for caries activity evaluation.

4.4. Molecular partner

This experiment identified 34 molecular companion peptide segments, belonging to the Hsp60 (GroEL) family, Hsp70 (DnaK) family, Hsp90 (Http pG) family, and Hspl00 (CIp) family. GroEL's E. coli is a homologous oligomer complex that plays an important role in the correct folding and assembly of newborn proteins and the recovery of degenerative proteins under thermal or chemical adversity. Although it has been determined that GroEL is located in the cytoplasm, the surface of some pathogens can express GroEL, and this is generally associated with the role the molecular partners play during adhesion [15]. GroEL expression was also detected in plaque fluid. It is speculated that the Hsp molecular companion, as the main antigen of most pathogens, may cause GroEL rearrangement on the bacterial cell membrane in the process of bacterial infection or under stress stimulation. Unlike the first two HSP, we found that HtpG was significantly upregulated in the CS group, but relevant studies showed that HSP90 synthesis speed and synthesis volume after stress were not significantly different than the above HSP, so its mechanism of cell protection needs to be further clarified.

4.5. Phosphorylation modification

In this experiment, the presence of two-component systems and Phosphotransferase system (PTS) was detected and consistently increased in expression in group CS, suggesting active protein phosphorylation modification and intercellular signaling in pathogenic biofilms.

The PTS system usually consists of five proteins including the enzyme I, enzyme (including three subunits of A, B and C) and phosphoolenol pyruvate (phosphoenolpyruvate, HPr). High expression of PTS system IIA, IIC in the CS group was also observed in this trial, indicating that the glucose intake within the flora was active during the occurrence of caries and development.

4.6. Bacterial phages

At present, specific phages for bacteria such as *Actinomyces, Actinobacillus Actinomycetecomitans, Actinomyces viscosus, Enterococcus faecalis (Actinomyces Actinobacillus actinomycetecomitans, Actinomyces viscosus, Enterococcus faecalis* have been isolated in plaque and saliva respectively, In this experiment, eight phage-related proteins were detected in two groups, two of them (phages and microstructural proteins) were highly expressed in the high caries group. Although less data on this finding is available, some scholars have speculated on the potential prospect of bacteriophages in the caries prevention and treatment process [16–19]. Taking a phage as a plaque control method may be a new area.

4.7. Membrane protein

The outer membrane is the contact surface of the bacteria and the external environment, and its main components are lipid, lipoprotein and outer membrane protein. Outer membrane protein is the main component of the outer membrane, which plays an important role in material transport, information identification, cell adsorption, and outer membrane protein and secreted protein are also the first choice protein of vaccine antigens. A variety of high-expression of bacterial outer membrane protein, lipoprotein, and apolipoprotein were detected in this experiment, but its function in the occurrence and development of caries needs yet to be studied specifically.

4.8. Other key proteins

After PRM verification, we found some key proteins which may play an important role during the development of dental caries in children (Fig. 13), which are discussed below.

Our experimental results show that although PFK and PK are highly expressed in both CF, CS groups, it exceeds 1.5 times in the CS group, indicating that PEK and PK play an important role in the occurrence and development of caries, especially in bacterial caries, and also shows that the glycolysis process can provide energy for the life activity of bacterial cells and maintain the bacterial physiological function in mature plaque.

In addition, this experiment also found that glycan phosphate isomerase was highly expressed in the plaque fluid in children with high caries, indicating that this enzyme may play an important role in the plaque caries-causing process by promoting the effective energy generation of the plaque bacteria.

ADH is a zinc-containing metallicase widespread in human and animal liver, plant and microbial cells, with a broad substrate specificity to convert pyruvate produced by glycolysis into acetaldehyde and NAD and NAD$^+$, thereby generating the energy needed for glycolysis. In this experiment, we found that ADH was highly expressed in the high caries group. It remains to be further studied, whether it also plays a role in the caries-induced transformation of plaque and the information exchange between bacteria.

Hydrohydrogenase (hydrogenase) is an important class of biological enzymes present in the microorganisms that catalyze the oxidation of hydrogen or hydrogen production from reduced protons. In our experimental results, the presence of iron hydrogenase and ferroxygen reduction protein was detected in both groups and significantly highly expressed in the high caries group, presuming that this may be one of the mechanisms where acid-producing and acid-resistant bacteria survive in the acid-induced plaque.

In conclusion, in the present study, we obtained 1804 peptides with quantitative information, including 395 in CF group, 30 in CS group, 1735 peptides in both the groups. The DeCyder^{TM}MS software conducted further statistics and analysis, and obtained 603 data sets of different peptide expression. The function of 391 peptides was unknown in this experimental dataset, and 47 peptides were highly

expressed in the high caries group. Their specific function and their relationship with the caries are still uncertain. Nevertheless, macroproteomics, secretory proteomics and bioinformatics analysis has still provided a very good platform for our research, so that we could conduct a good comprehensive analysis of the proteins known to-date. Further research will be conducive to clarify the cause, and looking for disease-related biomarkers, which will be one of our future research directions.

Acknowledgments

Conflict of interest

None to report.

References

[1] Corby PM, Lyons-Weiler J, Bretz WA, et al. Microbial risk indicators of early childhood caries. J Clin Microbiol. 2005; 43: 5753-5759.
[2] Li Y, Ge Y, Saxena D, Caufield PW. Genetic profiling of the oral microbiota associated with severe early-childhood caries. J Clin Microbiol. 2007; 45: 81-87.
[3] Lin Y, Qiu L, Gao X. Relationship between protein components in saliva and plaque fluid and caries susceptibility. Chinese Journal of Stomatology. 2002; 37: 39-42.
[4] Yao Y, Grogan J, Zehnder M, et al. Compositional analysis of human acquired enamel pellicle by mass spectrometry. Arch Oral Biol. 2001; 46: 293-303.
[5] Yao Y, Berg EA, Costello CE, et al. Identification of protein components in human acquired enamel pellicle and whole saliva using novel proteomics approaches. J Biol Chem. 2003; 278: 5300-5308.
[6] Liu Z. Oral biology. People's Health Publishing Company. Third edition.
[7] Hillman JD, Brooks TA, Michalek, et al. Construction and characterization of an effector strain of *Streptococcus mutans* for replacement therapy of dental caries. Infect Immun. 2000; 68: 543-549.
[8] Fitzgerald RJ, Adams BO, Sandham HJ, et al. Cariogenicity of a Lactate dehydrogenase-deficient mutant of *Streptococcus mutans* serotype c in gnotobiotic rats. Infect Immun. 1989; 57: 823-826.
[9] Hillman JD. Lactate dehydrogenase mutants of *Streptococcus mutans*: isolation and preliminary characterization. Infect Immun. 1978; 21: 206-212.
[10] Yang D, Liu T, Zhou X, et al. Preliminary study on LDH activity of Streptococcus mutans isolates from different caries sensitive populations. West China Journal of Stomatology. 2005; 23: 116-118.
[11] Zhu GP, Golding GB, Dean AM. The selective cause of an ancient adaptation. Science. 2005; 307: 1279-1282.
[12] Lunzer M, Mill ER SP, Felsheim R. The biochemical architecture of an ancient adaptive landscape. Science. 2005; 310: 499-501.
[13] Ell-ington AD, Bull JJ. Changing the cofactor diet of an enzyme. Science. 2005; 310: 454-455.
[14] Jung IL, Kim SK, Kim IG. The RpoS-mediated regulation of isocitrate dehydrogenase gene expression in *Escherichia coli*. Curr Microbiol. 2006; 52: 21-26.
[15] Garduno RA, Garduno E, Hoffman PS. Surface-associated hsp60 chaperonin of *Legionella pneumophila* mediates invasion in a HeLa cell model. Infect Immun. 1998; 66: 4602-4610.
[16] Delisle AL, Nauman RK, Minah GE. Isolation of a bacteriophage for *Actinomyces viscosus*. Infection and Immunity. 1978; 20: 303-306.

[17] Tylenda CA, Calvert C, Kolenbrander PE, Tylenda A. Isolation of *Actinomyces* bacteriophage from human dental plaque. Infection and Immunit. 1985; 49: 1-6.
[18] Yeung MK, Kozelsky CS. Transfection of *Actinomyces* spp. by genomic DNA of bacteriophages from human dental plaque. Plasmid. 1997; 37: 141-153.
[19] Bachrach G, Leizerovici-Zigmond M, Zlotkin A, Naor R, Steinberg D. Bacteriophage isolation from human saliva. Lett Appl Microbiol. 2003; 36: 50-3.